JOURNAL OF GEOPHYSICAL RESEARCH, VOL. 114, D14101, doi:10.1029/2008JD011639, 2009

Solar trends and global warming

R. E. Benestad[1] and G. A. Schmidt[2]

Received 17 December 2008; revised 27 April 2009; accepted 13 May 2009; published 21 July 2009.

[1] We use a suite of global climate model simulations for the 20th century to assess the contribution of solar forcing to the past trends in the global mean temperature. In particular, we examine how robust different published methodologies are at detecting and attributing solar-related climate change in the presence of intrinsic climate variability and multiple forcings. We demonstrate that naive application of linear analytical methods such as regression gives nonrobust results. We also demonstrate that the methodologies used by Scafetta and West (2005, 2006a, 2006b, 2007, 2008) are not robust to these same factors and that their error bars are significantly larger than reported. Our analysis shows that the most likely contribution from solar forcing a global warming is 7 ± 1% for the 20th century and is negligible for warming since 1980.

Citation: Benestad, R. E., and G. A. Schmidt (2009), Solar trends and global warming, *J. Geophys. Res.*, *114*, D14101, doi:10.1029/2008JD011639.

1. Introduction

[2] The Intergovernmental Panel on Climate Change (IPCC) report of 2007 assessed that the change in solar radiative forcing (henceforth referred to as "solar forcing") over the interval 1750–2005 was likely to be in the range $0.12–0.30 \mathrm{Wm}^{-2}$, compared to the total net anthropogenic forcing $1.7 \mathrm{Wm}^{-2}$ ($0.6–2.4 \mathrm{Wm}^{-2}$ [*Solomon et al.*, 2007]). However, detection and attribution of climate change related to long-term solar variability remains a contentious subject, with vastly different estimates appearing in the literature for the 20th century and for more recent decades [e.g., *Lean and Rind*, 2008; *Bard and Delaygue*, 2007; *Lockwood and Fröhlich*, 2007; *Lean*, 2006; *Scafetta and West*, 2005, 2006a, 2006b, 2007, 2008; *Douglass and Clader*, 2002; *Benestad*, 2002; *Stott et al.*, 2001].

[3] In particular, *Scafetta and West* [2006a, henceforth "SW06a"] claim that between 25 and 35% of the increase in the global mean temperature $\langle T \rangle$ since 1980 can be attributed changes in the solar activity. Note that the 25% and 35% attribution in SW06a was not the range including uncertainties, but their "best" estimates using either ACRIM or PMOD composites of total solar irradiance observations. The actual range including uncertainties would have been much wider. These estimates strongly contrast with independent work indicating that there is no significant trend in the solar activity since 1952, implying that there is no basis for any solar-induced trend since that time [*Benestad*, 2005; *Richardson et al.*, 2002; *Lean*, 2006; *Lockwood and Fröhlich*, 2007].

[4] More recently, *Scafetta and West* [2007, 2008] presented new calculations from which they concluded that solar forcing may have contributed with as much as 50% or 69% of the observed global temperature increase since 1900. Their research uses a so-called "phenomenological" method based on a fitting procedure to spectral data. Such a large role for solar activity in the warming since 1900 would imply that attribution studies for that period might need to be revisited, but doesn't necessarily imply that the effects of greenhouse gas changes in the future would be affected since uncertainties in the total forcings (including aerosol effects) preclude using the 20th century as a strong constraint on overall climate sensitivity [*Annan and Hargreaves*, 2006].

[5] Here we try to shed more light on the role of solar forcing by investigating the solar signal in a set of global climate model (GCM) simulations, and then comparing these with corresponding analysis based on the observed temperature record. A suite of 20th century simulations has been performed with GISS ModelE GCM, driven with a full range of estimated forcings over this period as well as with each individual forcing separately [*Schmidt et al.*, 2006; *Hansen et al.*, 2007]. This is a perfect test bed for the various methods, since the "true" amount of solar contribution in each experiment is already known and the amount of interannual "weather noise" and confounding effects (internal variability and response to other forcings) are close to observed.

[6] The error bars on the attribution of the solar component between 1750 and 2005 inferred from IPCC are around 7 to 18% of the total forcing, though since that also includes a negative aerosol component, it might be clearer to say 4 to 11% of the forcings contributing to the warming (including well-mixed greenhouse gases, ozone and black carbon). A full detection and attribution analysis can take into account possible underestimates of the solar forcing and potentially a difference in sensitivity for different forcings (the "efficacy" [*IDAG*, 2005]). The inferred error bars in the IPCC report do not span the results claims by Scafetta and West, and so there may be systematic issues with the different

[1]Climate Division, Norwegian Meteorological Institute, Oslo, Norway.
[2]NASA Goddard Institute for Space Studies, New York, New York, USA.

0148-0227/09/2008JD011639$09.00

Table 1. Data Sources

CO_2	http://cdiac.ornl.gov/ftp/trends/co2/maunaloa.co2
Lean [2000]	ftp://ftp.ncdc.noaa.gov/pub/data/paleo/climate_forcing/solar_variability/lean2000_irradiance.txt
Lean et al. [1995]	ftp://ftp.ncdc.noaa.gov/pub/data/paleo/contributions_by_author/lean1995/irradiance_data.txt
Obs. $\langle T \rangle$	http://data.giss.nasa.gov/gistemp/graphs/Fig.A2.txt
PMOD	http://www.pmodwrc.ch/dat/composite_d19.asc
GISS forcings	http://data.giss.nasa.gov/modelforce/RadF.txt

approaches that have not been sufficiently addressed. In order to help resolve this question, we repeat the analyses of Scafetta and West (hereafter SW) and compare them with a suite of independent analyses, both over the observational data and model-generated analogs to test their robustness. The paper is divided into 2 parts, of which the first explores the danger of applying linear statistical methods to data from a complicated and chaotic system. The second part repeats the analyses of SW to explore whether similar problems can affect their results.

2. Data

[7] We focus on the forcings and responses of the climate over the 20th century. The solar forcing in these analyses is characterized by the total solar irradiance (henceforth denoted by "S") and its spectral changes. We use the S reconstruction from *Lean* [2000] initially for compatibility to what was used in model experiments performed in 2004. More recent estimates of solar forcing have a smaller long-term trend [*Foukal et al.*, 2006; *Wang et al.*, 2005], so the use of the older forcing would tend to increase the attribution to solar in our analyses. The impact of different estimates is addressed in later sensitivity tests. The observed global mean temperature was taken from NASA GISTEMP product [*Hansen et al.*, 2001, and updates], though the results are insensitive to the choice of a different temperature data set (i.e., HadCRUT3v [*Brohan et al.*, 2006]). Other forcings including well-mixed greenhouse gases, aerosols, volcanoes, land use and tropospheric and stratospheric ozone for the 20th century are outlined by *Hansen et al.* [2006].

[8] Ensemble simulations, each of 5 members, were performed with GISS ER for experiments with different sets of forcings: All natural and greenhouse gas concentrations ("all"), solar forcing only ("solar"), and greenhouse gases only ("GHG"). The equilibrium climate sensitivity of GISS ModelE is 2.7°C for a doubled atmospheric concentration of CO_2, whereas the transient response at the time of CO_2 doubling in a 1% increasing CO_2 experiment is 1.6°C [*Solomon et al.*, 2007, Table 8.2]. Data sources and details about the data are listed in Tables 1 and 2.

3. Part 1: Multiple Linear Regressions

3.1. Methods

[9] We first analyze the annual and global mean temperature (henceforth referred to as "$\langle T \rangle$") together with various estimates of changes in the external forcings. Here the notation $\langle x \rangle$ for an arbitrary variable x (in this case temperature) means the spatial mean of the variable x (such as the global mean), whereas $\bar{x}$ will be used to represent the temporal mean (over the entire time interval). Furthermore, $\hat{x}$ is used to represent the estimated value of x.

[10] The analysis involves several independent assessments, including trend analysis, lagged correlation functions (LCFs), and various regression exercises.

[11] The regression analysis [*Lean and Rind*, 2008; *Camp and Tung*, 2007; *Ingram*, 2006] should in this context be regarded as a naive approach that is prone to yielding biased results, and we caution against using such techniques without a critical interpretation. Here we use the regression to demonstrate how spurious results may arise from colinearity and "noise" by examining the variability in the coefficients, which has a direct relevance to the analysis in part 2. The regression coefficients represent the weights of a combination of the forcings that gives the closest description of $\langle T \rangle$ (smallest errors), and thus provide the best estimate of the magnitude of the response to the different forcings in both experiments and observation. In other words, the regression analysis in this case merely provides a crude "yard stick" for the temperature response to various forcings that enable a simple comparison between model and observations.

[12] First, an ordinary linear regression (OLR) analysis is employed to estimate the linear sensitivity of $\langle T \rangle$ to S and the CO_2 concentrations (ρ in ppm), ignoring all other factors:

$$\langle \hat{T} \rangle = \alpha_0 + \frac{0.7}{4}\alpha_1 S + 5.35\alpha_2 \times \ln(\rho) + \eta. \quad (1)$$

[13] The values of S were scaled by 0.7/4 to get the equivalent forcing to account for the Earth's geometry and albedo (taken to be 0.3), and a scaling constant of 5.35 W/m^2 was used for the logarithmic relationship with CO_2 in order to get equivalent units for the GHG forcings [*Myhre et al.*, 1998]. The last term in equation (1), η, describes variability not related to solar forcing or GHGs (here referred to as "noise").

[14] The coefficients α_1 and α_2 can be associated with the transient climate sensitivity and are expected to have similar values.

[15] There are also a number of other forcings that may influence the climate that were not included above. Thus to explore whether neglected forcings could affect the results [*Lean and Rind*, 2008] and to expand the analysis to include longer time series, we compared $\langle T \rangle$ with a full set of known forcings used in the GISS model experiments [*Hansen et al.*, 2005]. The effects of these forcings on the temperature were to a first-order described in equation (2):

$$\langle \hat{T} \rangle = \beta_0 + \beta_1 F_S + \beta_2 F_{GHG} + \beta_3 F_{O3} + \beta_4 F_{H2O} + \beta_5 F_{land} + \beta_6 F_{snow} + \beta_7 F_{Aer} + \beta_8 F_{BC} + \beta_9 F_{Refl} + \beta_{10} F_{AIE} + \eta, \quad (2)$$

Table 2. Identifiers for the GCM Experiments With GISS ModelE

"All forcings"	E3Af8a, E3Af8b, E3Af8c, E3Af8d, E3Af8e
Well-mixed "GHG"	E3GHGa, E3GHGb, E3GHGc, E3GHGd, E3GHGe
"Solar"	E3SOa, E3SOb, E3SOc, E3SOd, E3SOe
"CTL"	E3oM20

where F_S is the solar forcing at the top of the atmosphere ($F_S = 0.7/4 \times S$), F_{GHG} describes radiative forcing due to well-mixed GHG concentrations, F_{O3} describes forcing due to stratospheric ozone, F_{H2O} represents stratospheric moisture, F_{Refl} reflective tropospheric aerosols, F_{land} landscape changes (land use), F_{snow} snow albedo (black carbon effect), F_{Aer} represents stratospheric aerosols (volcanoes), F_{BC} is black carbon, F_{AIE} is aerosol indirect effect (e.g., through cloud drop modification), and η is a noise term. These forcings are discussed further by *Hansen et al.* [2005], and were the same as those used as boundary conditions in the "all" simulations. This set of forcings hence provided an opportunity to compare response of the observed $\langle T \rangle$ with simulations where the response is determined from the formulation of the physical processes thought to be involved.

[16] The coefficients in equation (2) were estimated through a stepwise multiple regression to avoid overfitting, and the values of these are expected to reflect the climate sensitivity of the model. Weak signals may not be detected as the response may be swamped by internal variations, but values that are physically unreasonable will identify these cases.

[17] The stepwise screening used the Akaike information criterion (AIC [*Wilks*, 1995, pp. 300–302]) to determine which forcings to include, and a Durbin-Watson test was applied to check the regression analysis to indicate the potential presence of autocorrelation in the residuals.

[18] We do find nonzero autocorrelation in the residuals, suggesting that the regression was not optimal and that the significance levels and error bars derived by the regression analysis are too conservative. However, the objective of the regression in this case is to provide a means of comparing the relative magnitude of the response to the different forcings. We also want to explore how the coefficients for the terms in equation (2) are affected by unrelated forcings, to check how robust the regression analysis was with respect to colinearity and the presence of internal chaotic variations, and thus whether the regression analysis could give misleading results due to unrelated signals or errors. If the coefficients from the regression are spuriously inflated, then unrelated forcings project onto the solutions, and that has direct relevance for the studies discussed in part 2.

3.2. Results

3.2.1. Lag Correlation Analysis

[19] Figure 1 shows the LCF between the annual mean value for $\langle T \rangle$ and *Lean* [2000] S, for the actual observations (a) as well as the "all" (b), "GHG" (c) and "solar" (d) ensemble means. The LCF for S and $\langle T \rangle$ for the observed temperature suggested a response to solar forcing that is strongest when $\langle T \rangle$ leads S by zero to one year. SW06a, on the other hand, assumed 1.3 years, 2.5 years, and 4.3 years lags for the 11-year, 22-year, and longer timescales respectively, based on *Wigley* [1988], and combined these in a single equation describing the temperature response.

[20] The corresponding LCF for "all" also indicates that the $\langle T \rangle$ leads S by approximately one year, albeit with similar but marginally lower correlation for zero lag. The lag correlation peaks when $\langle T \rangle$ lags S by one year in the case of the "solar" experiment, but the structure for "GHG" appears to phase shifted with $\langle T \rangle$ leading S by 2 years or lagging by ~8 years. As expected, the phase relationship is not preserved when S was not included as a boundary condition in the numerical experiments.

[21] It is interesting, however, to note the time lag structures (i.e., the number of years between each lag correlation peak) in the LCFs with an apparent periodicity of ~9–10 years, rather than ~11 years, and that the variations in $\langle T \rangle$ appear to take place before similar fluctuations in S. These characteristics appear to be due to intrinsic variations rather than a common 11-year cycle (Figure 1c), since the solar cycle length has predominantly been longer than 10 years over the period 1880–2000 [*Benestad*, 2005, Figure 2]. These features may therefore suggest that the lagged correlation picks up a ringing effect arising from two slightly different frequencies. Such spurious phenomena may also result in inflated regression coefficients. Nevertheless, the results from the lag correlation analysis suggest that the solar signal is weak but present in both the observations and the GCM "all" results.

3.2.2. Solar Forcing and CO_2

[22] Figure 2 shows the time evolution of $\langle T \rangle$ of the "all" ensemble mean (blue thick line) and the corresponding observations (red thick line). It is evident that the time evolution for the two shows a high degree of coherence.

[23] We apply a regression analysis to compare the relative strength of the linear response to the solar and GHG forcings in the experiments and the observations, in order to provide further model evaluation and compare the influence of the different forcings. Due to the lagged response identified by the LCFs, the regression was applied to the forcings and $\langle T \rangle$ with no lag and with $\langle T \rangle$ lagging the forcing by one year.

[24] The analysis with only S and CO_2 concentrations as inputs in equation (1) (1958–2000), yielded the coefficients $\hat{\alpha}_1 = 0.48 \pm 26$ K/[Wm^{-2}] for the observations and $\hat{\alpha}_1 = 0.49 \pm 0.22$ K/[Wm^{-2}] for "all" (Table 3). Likewise, the corresponding coefficients for ln(CO_2) term are: $\hat{\alpha}_2 = 0.49 \pm 0.06$ K/[Wm^{-2}] for the observations and $\hat{\alpha}_2 = 0.43 \pm 0.05$ K/[Wm^{-2}] for "all" respectively. The results for zero lag were similar (Table 3), and suggest $\hat{\alpha}_1 \approx \hat{\alpha}_2$, hence that the climate sensitivity is similar for both solar and GHG forcing. Thus the transient climate sensitivity estimated for this model suggests that:

$$\frac{\Delta \langle T \rangle}{\Delta F_{TOA}} \approx 0.45 \text{ K}/\left[\text{Wm}^{-2}\right]. \quad (3)$$

[25] Furthermore, the similarity in results for the observations and "all" indicates that the GCM simulation of the response to these forcings is realistic. The regression provides a statistical model for $\langle T \rangle$ based on the historical forcings that was capable of reproducing the past temperature trends, both for the observations as well as for the simulations (Figure 1; red and blue open symbols for observations and "all" respectively).

[26] The regression was repeated for the GCM experiments "solar" and "GHG". The results for "all" give larger values for α_1 than for both the "solar" and "GHG" simulations (Table 3). For the latter, the coefficient should be zero but the estimated value was -0.11 ± 0.06 K/[Wm^{-2}] with the value of zero barely within the two-sigma estimate

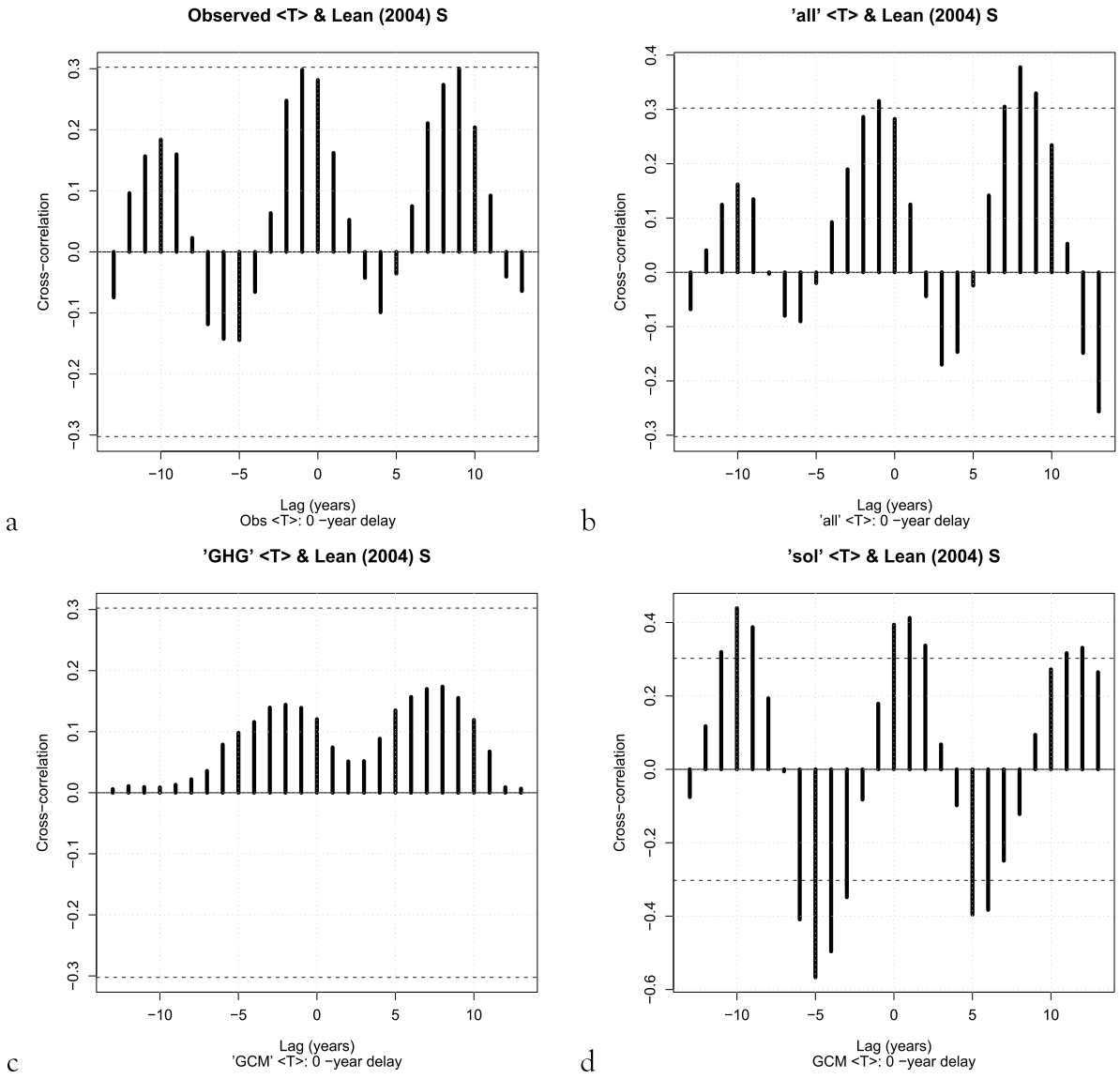

Figure 1. LCFs for temperature and *S*. (a) Observed, (b) "all," (c) "GHG," (d) "solar".

of the coefficient. This may suggest a nonlinear response to the combined natural and GHG forcings, however, a similar analysis for the residual ("res" = "all" – "GHG") gave negative values for $\hat{\alpha}_2$. The negative value may have been a result of increased aerosol loading associated with higher GHG forcing in the "all" simulations (Figure 3).

[27] The results from such naive regression analyses may also be misleading due to convoluted nonlinear response associated with feedback processes, nonoptimal regression, and colinearity [*Lean and Rind*, 2008]. To test how robust the method was with respect to a number of arbitrary choices, we repeated the regression analysis with only one input variable by excluding the $\ln(\rho)$ term in equation (1) (univariate regression). This time the values for α_1 for the observations and "GHG," were substantially higher than $\hat{\alpha}_1$ for the multiple regression (Table 3).

[28] Furthermore, there was less similarity between the univariate $\hat{\alpha}_1$ for the observations and "all" than in the multiple regression, and the difference between corresponding coefficients in the two regression exercises is because the two forcings are not orthogonal. These results indicated that the analysis only gave a consistent picture if all important forcings were accounted for, which is also true for the analysis presented in part 2 of this paper.

3.2.3. Full Set of Known Forcings

[29] The best fit derived from the stepwise multiple regression (equation (2)) is shown as solid circular symbols in Figure 2, and trends from actual observations were compared with the "all" experiment ensemble mean. The "all" results provide a similar trend estimate as the observations, but the "solar" results indicate that little warming over the 1960–2000 period can be attributed to changes in the sun (Figure 2, gray curve). Table 4 shows the results for the multiple regression analysis based on the ten GISS forcings over the interval 1880–2002. The analysis was also applied to the ensemble means of "GHG" and "solar" to provide a reference, as we have *a priori* knowledge about

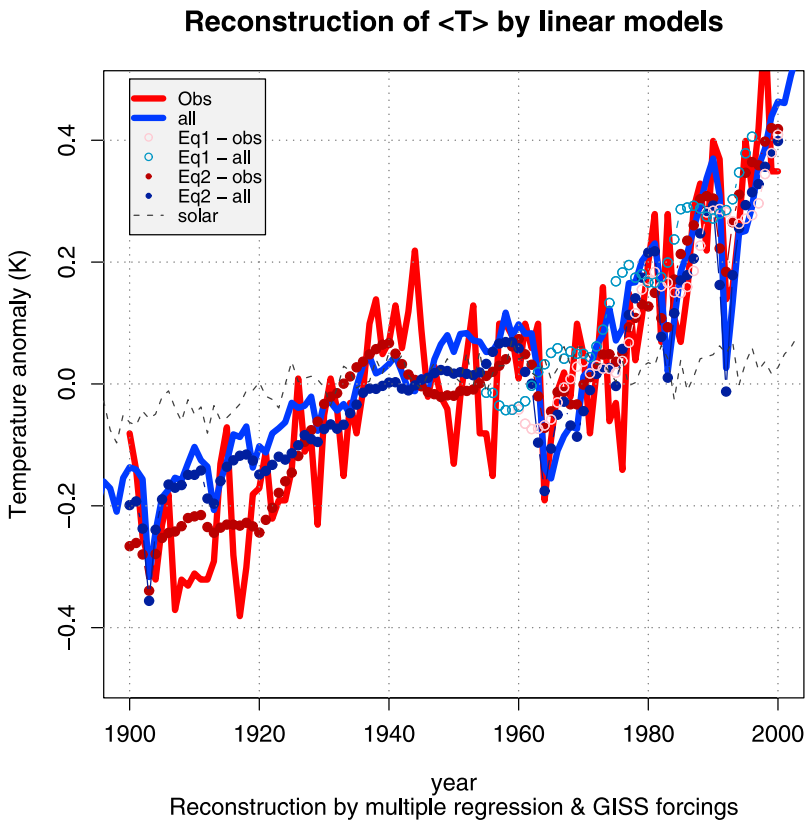

Figure 2. Observed $\langle T \rangle$ and "all" (thick curves), together with predictions based on equation (1) (open circles) and linear multiple regression models in equation (2) using all known forcings as input (solid circles).

the role of the forcings in these experiments. The analysis for a 1-year lag gave small values for β_1 with both the "solar" simulations (0.08 ± 0.05 K/[Wm^{-2}]; not shown) and observations (0 K/[Wm^{-2}]; excluded by the stepwise screening), but a higher value with "all" (0.40 ± 0.16 K/[Wm^{-2}]). The latter value suggests a climate sensitivity that is of similar magnitude to that derived from the regression analysis based on just solar forcing and CO_2 (equation (3)). However, the GCM seems to be somewhat more sensitive to changes in F_S than the observations and less sensitive to F_{GHG}.

[30] The results for the ensemble means are not directly comparable to the observations, since the historical measurements are the equivalent a single realization, i.e., an arbitrary component of internal chaotic variations superimposed on the forced response. Thus whereas the ensemble means will emphasize the common signal due to the forcing, the regression results with the observed data should really be compared with the range derived from the different ensemble members. For the "all" experiment, the regression coefficients associated with F_S and F_{GHG} are $\hat{\beta}_1 = 0.36-0.61$ ($\pm\sim 0.19$) K/[Wm^{-2}] and $\hat{\beta}_2 = 0.26-0.70$ ($\pm\sim 0.19$) K/[Wm^{-2}] respectively. The results for the observations, on the other hand, give $\hat{\beta}_1 = 0$ K/[Wm^{-2}] and $\hat{\beta}_2 = 0.91 \pm 0.19$ K/[Wm^{-2}]. In this case, the β_2 estimate for the observations implies unrealistically high climate sensitivity, due to the exclusion of F_S in the stepwise screening. It is possible that errors in F_S may have wrongly caused solar forcing to fail the screening test.

[31] The value for β_2 of the "GHG" runs (0.26 ± 0.03 K/[Wm^{-2}]; not shown) is lower than those obtained for the "all" ensemble mean (0.57 ± 0.17 K/[Wm^{-2}]) and individual members ($0.26-0.70$ K/[Wm^{-2}]), but the estimates for β_2 are associated with small error bars. The solar terms, on the other hand, are associated with relatively large error estimates, implying a larger sensitivity to the internal variability.

Table 3. Regression Coefficients Obtained Through Regression Analyses (Units in K/[Wm^{-2}])[a]

	Univariate Solar Coefficient $\hat{\alpha}_1$	Multiple Solar Coefficient $\hat{\alpha}_1$	GHG Coefficient $\hat{\alpha}_2$
		Lag 0	
Obs	0.69 ± 0.40 (0.09)	0.44 ± 0.25 (0.09)	0.51 ± 0.06 (0.00)
All	0.21 ± 0.02 (0.00)	0.39 ± 0.22 (0.08)	0.48 ± 0.05 (0.00)
Solar	0.05 ± 0.00 (0.00)	0.15 ± 0.05 (0.01)	−0.01 ± 0.01 (0.50)
Res	−0.10 ± 0.02 (0.00)	0.50 ± 0.24 (0.04)	−0.31 ± 0.06 (0.00)
GHG	0.31 ± 0.03 (0.00)	−0.11 ± 0.06 (0.07)	0.79 ± 0.01 (0.00)
		Lag 1 year	
Obs	0.72 ± 0.39 (0.07)	0.48 ± 0.26 (0.07)	0.49 ± 0.06 (0.00)
All	0.21 ± 0.02 (0.00)	0.49 ± 0.22 (0.03)	0.43 ± 0.05 (0.00)
Solar	0.05 ± 0.00 (0.00)	0.07 ± 0.06 (0.25)	−0.01 ± 0.01 (0.71)
Res	−0.10 ± 0.02 (0.00)	0.66 ± 0.23 (0.01)	−0.36 ± 0.06 (0.00)
GHG	0.31 ± 0.03 (0.00)	−0.16 ± 0.06 (0.01)	0.79 ± 0.01 (0.00)

[a]The rows presents the results for the ensemble means for the "all," "solar," "residual," and "GHG," respectively. The numbers in the parentheses are the p values (assuming independent data) associated with the regression results.

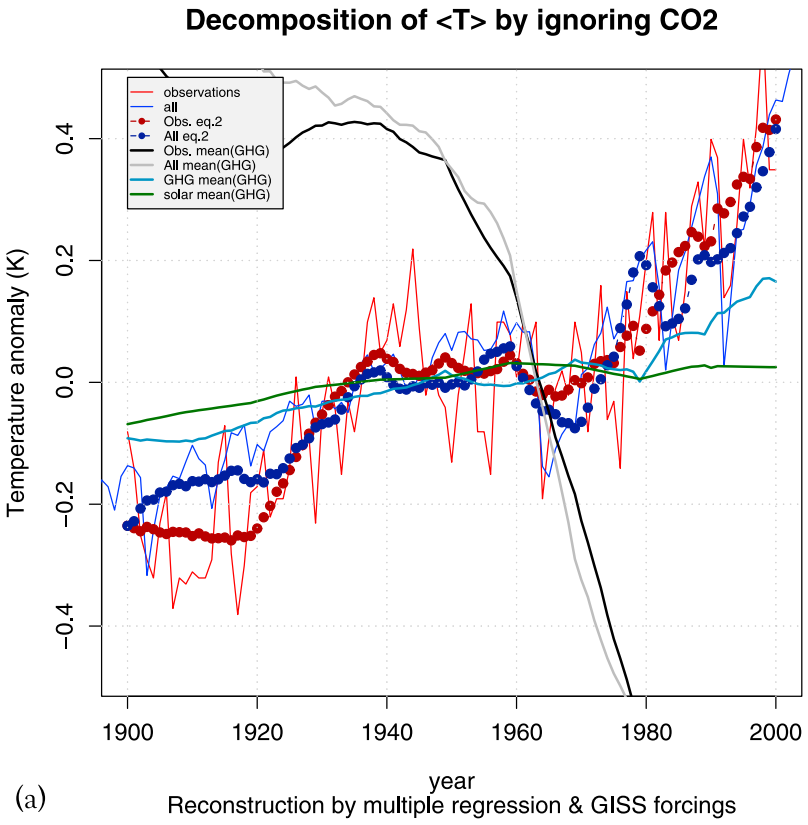
Decomposition of <T> by ignoring CO2
observations
all
Obs. eq.2
All eq.2
Obs. mean(GHG)
All mean(GHG)
GHG mean(GHG)
solar mean(GHG)
Temperature anomaly (K)
0.4
0.2
0.0
−0.2
−0.4
1900
1920
1940
1960
1980
2000
year
Reconstruction by multiple regression & GISS forcings

(a)

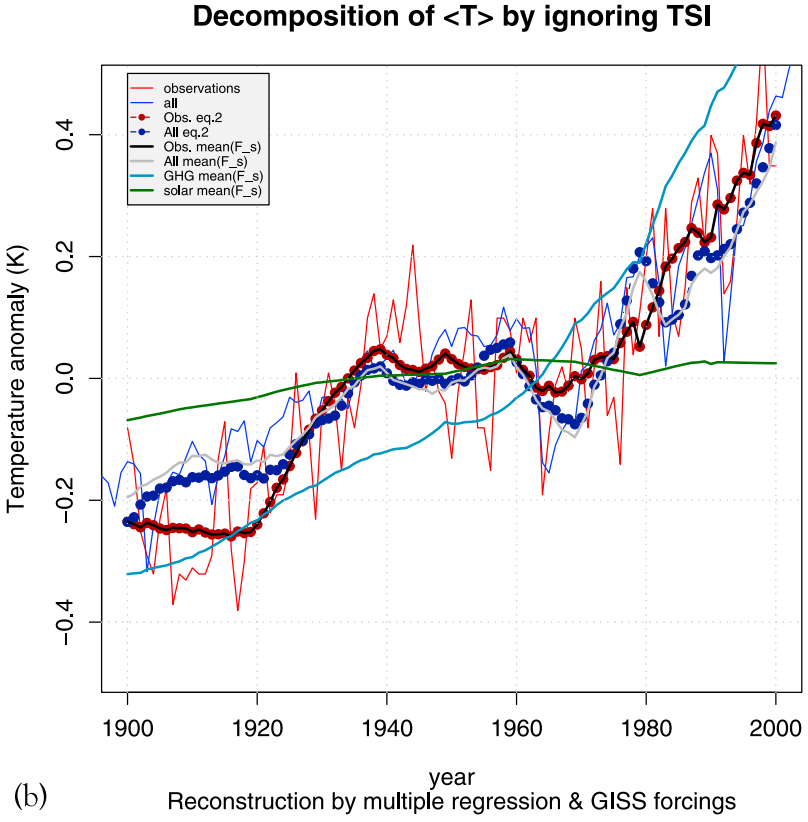
Decomposition of <T> by ignoring TSI
observations
all
Obs. eq.2
All eq.2
Obs. mean(F_s)
All mean(F_s)
GHG mean(F_s)
solar mean(F_s)
Temperature anomaly (K)
0.4
0.2
0.0
−0.2
−0.4
1900
1920
1940
1960
1980
2000
year
Reconstruction by multiple regression & GISS forcings

(b)

Figure 3

Table 4. Regression Coefficients Obtained Through Multiple Regression on the GISS Forcings Estimates (Units in K/[Wm^{-2}])[a]

	Lag = 0 year, Obs.	Lag = 1 year, Obs.
Const (β_0)	−0.18 ± 0.034***	−0.22 ± 0.03***
Solar (β_1)		
GHG (β_2)	0.95 ± 0.18***	0.91 ± 0.19***
Ozone (β_3)	7.45 ± 3.26*	8.10 ± 3.35*
Vapor (β_4)		
Land (β_5)	−21.14 ± 6.44**	−18.12 ± 6.60**
Snow (β_6)	−14.44 ± 7.43.	−18.79 ± 7.62*
Aerosol (β_7)	0.04 ± 0.02*	
Black C (β_8)	11.58 ± 4.16**	13.18 ± 4.27**
Reflect. (β_9)	4.72 ± 1.83*	5.35 ± 1.88**
Indirect (β_{10})	4.37 ± 1.77*	3.26 ± 1.79.
	RSE: 0.09 on 115 *df* MRS: 0.85, ARS: 0.84. *F*: 79.84 on 8 and 115 *df*, p < 2.2e−16.	RSE: 0.09 on 115 *df* MRS: 0.83, ARS: 0.82. *F*: 79.78 on 7 and 115 *df*, p < 2.2e−16
	Lag = 0 year, "all"	Lag = 1 year, "all"
Const (β_0)	−0.14 ± 0.02***	−0.26 ± 0.03***
Solar (β_1)	0.34 ± 0.11**	0.40 ± 0.16*
GHG (β_2)	0.30 ± 0.08***	0.57 ± 0.17***
Ozone (β_3)	−2.11 ± 0.69**	−2.50 ± 1.06*
Vapor (β_4)		−29.64 ± 17.39.
Land (β_5)	−2.22 ± 0.82**	
Snow (β_6)	−6.06 ± 1.44***	−12.86 ± 3.40***
Aerosol (β_7)	0.12 ± 0.01***	
Black C (β_8)		
Reflect. (β_9)	−0.80 ± 0.45.	−1.67 ± 1.01
Indirect (β_{10})		−2.03 ± 0.43***
	RSE: 0.05 on 116 *df* MRS: 0.94, ARS: 0.94. *F*: 265.5 on 7 and 116 *df*, p < 2.2e−16	RSE: 0.07 on 115 *df* MRS: 0.86, ARS: 0.85. *F*: 100.5 on 7 and 115 *df*, p < 2.2e−16

[a]The rows present the results for the ensemble means for the "all" and the observed temperatures. Signif. codes: "***" 0.001, "**" 0.01, "*" 0.05, "." 0.1, " " 1. Abbreviations: RSE, residual standard error; MRS, multiple residual squared; ARS, adjusted R^2; *df*, degrees of freedom; *F*, *F* statistic; *p*, *p* value.

[32] The estimates for many of the weak forcings give high values that are difficult to explain in terms of physics (β_3–β_{10} in Table 4). Thus the results suggest that it is difficult to detect any response to these in $\langle T \rangle$. These results also highlight the danger of attributing signal to forcings with similar characteristics, which is also the shortcomings of the studies discussed in part 2.

[33] Figure 3a shows predictions with the regression model described by equation (2), where the effect of GHGs have been removed by setting their concentration $F_{GHG} \rightarrow \overline{F_{GHG}}$ while including the time dependency for the other forcings (all the coefficients β_0–β_{10} being the same as previously). Hence the regression model is the same as before, but by including or excluding different forcings, the effects from the different forcings are compared. The statistical model predictions suggested a cooling if the effect of GHGs was removed (thin black or blue dashed curves); a similar result to that seen in the IPCC report [*Hegerl et al.*, 2007, Figure 9.5]. The pronounced downturn in the predicted values with $F_{GHG} \rightarrow \overline{F_{GHG}}$ after 1940 (thin black and blue dashed lines in Figure 3a) can be explained by exaggerated values for β_3–β_{10} and increasing negative forcings.

[34] If the solar contribution is ignored by setting $F_S \rightarrow \overline{F_S}$, this makes little difference compared to the full multiple regression (Figure 3b, thin black and blue dashed). The solar contribution to the most recent warming was estimated by setting all of the inputs in the multiple regression models (equation (2)) to their mean value, except for the solar forcing, using these together with the regression models, and applying a simple linear trend analysis to the predicted temperatures. This gave a zero slope for the observations over the interval 1900–2000, and 11.5 ± 9.7% of the observed warming for "all" (not shown).

[35] Figure 3 also shows the corresponding analysis done for "GHG" (thin red dashed) and "solar" (thin green dashed). None of these experiments, however, reproduced the observed time evolution for the temperature. The "GHG" analysis exhibited an upward trend between 1880–2000 in Figure 3a (red dashed line), despite $F_{GHG} \rightarrow \overline{F_{GHG}}$, but the "solar" analysis shows a weak upward evolution in Figure 3b too (green dashed line), even when the effect of F_S is excluded in the regression analysis. This sensitivity to unrelated forcings can be explained by a similar trend in both.

Figure 3. Simulations (solid lines) and predictions (dashed lines) of global mean temperature, the latter based on multiple regression (equation (2)) masking out either F_S or F_{GHG}. (a) Predictions based on multiple regression against GISS forcings used in the all experiments (thick dashed), together with predictions based on the multiple regression model (thin dashed) where changes in the concentration of the greenhouse gases have been excluded ($F_{GHG} \rightarrow \overline{F_{GHG}}$). (b) Same as in Figure 3a, but the influence of TSI has been excluded ($F_S \rightarrow \overline{F_S}$) instead of greenhouse gases. Note, "Obs. mean (F_s)" is hidden behind another line as $\beta_1 = 0$ in this case.

[36] If only F_S and F_{GHG} from the GISS forcings are used in equation (2) and the other terms ignored in the regression model calibration, then the analysis returned similar results for the observations and "all" (over the interval 1880–2002 and 1-year lag, $\hat{\beta}_1 = 0.54 \pm 15$ K/[Wm^{-2}] and $\hat{\beta}_2 = 0.19 \pm 0.02$ K/[Wm^{-2}] for the observations whereas "all" gave 0.63 ± 0.12 K/[Wm^{-2}] and 0.14 ± 0.01 K/[Wm^{-2}] respectively). Now the estimate for the climate sensitivity was greater for the solar forcing, and the results contrasted with $\hat{\beta}_1 = 0$ K/[Wm^{-2}] for the observations with the full set of forcings. The regression results were similar when the same test was repeated for the 1958–2000 interval.

[37] These results differed with the results derived using equation (1), as excluding all but solar and GHG from the GISS set of forcings gave stronger weight to the solar component. Thus colinearity, forcing differences, and unrelated internal chaotic variations always have an impact on identifying the response to forcings, whereas the choice of interval plays only a minor role in the differences in these regression results. The trend analysis of the regression models can be compared with the trends in the ensemble means of the GCM experiments. The 1900–2000 change in the ensemble mean for "solar" was estimated to be 0.1 ± 0.01K (here expressed as ± 1 standard deviation) compared to 0.57 ± 0.04K in the observations, 0.40 ± 0.03K in "all," and 0.79 ± 0.03K in "GHG". Thus the solar forcing contributed with 12.61 ± 9.31% of the forcing compared to greenhouse gases, but could account of 24.63 ± 10.7% of the change in "all," where additional forcings lower the net effect (which would also reduce the impact of solar activity). Over the 1980–2003 period, GISTEMP suggested a global warming of 0.39 ± 0.07K whereas "all" suggested 0.22 ± 0.06K, "GHG" 0.49 ± 0.02K, and "solar" 0.02 ± 0.02K. Thus the GCM simulations suggest that the solar trend over the last period does not differ from zero by more than one standard deviation.

4. Part 2: Scafetta and West Methodologies

4.1. Methods

[38] In this section, we analyze the GCM experiments with so-called "phenomenological" methods proposed by *Scafetta and West* [2006a, 2006b; hereafter SW06a and SW06b]. We repeated the analysis in SW06a and SW06b, and tested the sensitivity of the conclusions to a number of arbitrary choices. The methods of SW06a and SW06b were used (1) with the results from the GCM experiments with known forcings, (2) in sensitivity tests with different values in the model parameters or with different solar forcing proxies, (3) in Monte Carlo simulations, and (4) with spectral analysis.

[39] We reproduced the SW06a study, where changes in S were estimated by merging the estimates from *Lean et al.* [1995] and satellite measurements from *Fröhlich and Lean* [1998]. Here we choose to focus on the PMOD composite and examine SW06a's least extreme claim of a 25% temperature increase (since 1980) due to solar influences, rather than the ACRIM composite-based claim of a 35% attribution [*Willson and Mordvinov*, 2003]. The conclusions about the appropriateness of the methods does not hinge on the choice of PMOD (there is some contention about whether the PMOD is the most appropriate TSI representation, as *Lockwood and Fröhlich* [2008] conclude that the PMOD is more realistic than ACRIM, while *Scafetta and Willson* [2009] claim that the ACRIM composite is more realistic. However, the latter paper did not provide any detailed description of the method used to derive their results, and while they derived a positive minima trend for their composite, it is not clear how a positive minima trend could arise from a combination of the reconstruction of *Krivova et al.* [2007] and PMOD, when none of these by themselves contained such a trend), however, we used the following formula proposed by SW06a, relating $\langle T \rangle$ to the changes in the S for different timescales:

$$\langle \hat{T}_{sun} \rangle(t) = Z_{eq}\langle S_4(t) \rangle + Z_{S4}\left[S_4(t-\tau_{S4}) - \overline{S_4}(t)\right] + Z_{22y}D_4(t-\tau_4) + Z_{11y}D_3(t-\tau_3). \quad (4)$$

[40] S represents the total solar irradiance rather than the solar forcing at the top of the atmosphere ($S = 4/0.7 \times F_S$). The coefficients τ_{S4}(= 4.3 years), τ_4(= 2.5 years) and τ_3(= 1.3 years) describe a time-lagged response, supposedly representing the effect of thermal inertia associated with the world oceans. The variables $S_4(t)$, $D_4(t)$ and $D_3(t)$ are defined as the (wavelet) frequency band components of S, where $S_4(t)$ represented the long timescales (>22 years), whereas D_4 and D_3 describe the timescales 14.7–29.3 years (median 22yr) and 7.3–14.7 years (median 11yr) respectively. We use the "mra" function from the waveslim package for R to compute the wavelet components ("D = mra(y, wf = "la8", J = floor(log(length(y),2)), method = "modwt")", taking $D_4(t)$ = D$D8 and $D_3(t)$ = D$D7.), which should be similar to the algorithm used in the original analysis.

[41] Our analysis differs from that of SW06a by computing the linear trend as opposed to taking differences between filtered values at different times. Furthermore, the lagged response was estimated by employing cubic splines for interpolating the value at $t + \tau$, where τ was taken as lag in years (a fractional number). It is not clear how the lagged values were estimated by *Scafetta and West* [2006a], and the present reanalysis may differ slightly with their analysis in this respect.

[42] The coefficients Z_{11y} (referred to as "$Z_7 = A_{7,temp}/A_{7sun} = 0.11 \pm 0.02$ K/[Wm^{-2}]" in the work of *Scafetta and West* [2005], hereafter "SW05") and Z_{22y} (or "$Z_8 = A_{8,temp}/A_{8sun} = 0.17 \pm 0.06$ K/[Wm^{-2}]" in SW05) were estimated as the ratio of amplitudes A using "$f(t) = \frac{1}{2} A \sin(2 \pi t)$," but SW05 did not disclose how the frequency ω and phase information were accounted for. It is important to note that the wavelet components may not necessary be well represented by a sine function of a specific frequency. However, they used an expression $A = 2\sqrt{(2)}\ \sigma$, where $\sigma^2 = \frac{1}{T}\int_0^T [f(t) - \overline{f(t)}]^2\ dt$, so it is possible that they merely used the ratio $A_{temp}/A_{sun} = (2\sqrt{(2)}\ \sigma_{temp})/(2\sqrt{(2)}\ \sigma_{sun}) = \sigma_{temp}/\sigma_{sun}$. They estimated $A_{8,temp} = 0.06 \pm 0.01$K and $A_{8,sun} = 0.35 \pm 0.10$W/m^2.

[43] We nevertheless follow their procedure, and compare the ratio of the standard deviations of the corresponding wavelet components for the solar forcing and temperature respectively. In addition, the ratio was estimated more explicitly based on the value of A (we refer to this as A'), however, a robust conclusion should not be sensitive to

these choices. The latter involved the identification of a signal within a prescribed frequency band (using linear regression to estimate the coefficients):

$$\hat{D}_4 = \hat{\alpha}_c \cos(2\pi\omega t) + \hat{\alpha}_s \sin(2\pi\omega t), \quad (5)$$

where ω was chosen to represent a similar frequency as the filtered values (τ = 22 years), from which amplitude was given by the regression coefficients:

$$A' = \sqrt{\hat{\alpha}_c^2 + \hat{\alpha}_s^2}. \quad (6)$$

The estimation of the amplitude (equations (5) and (6)) was repeated for D_3 (τ = 11 years).

[44] The robustness of the SW06a method was tested against different realizations of intrinsic variability using individual ensemble members of the GCM experiments. Additionally, we calculated the null distribution for the amplitudes computed from two sets of Monte Carlo experiments, which in this case consisted of generating series using a random generator (1) to produce white noise with a normal distribution, and (2) generating random walk series where the steps were modeled as white noise. For both of these simulations, the standard deviation and mean of the series were set to same values as those for the observed data.

[45] The surrogate series in the Monte Carlo simulations were computed either (1) by taking the differences between two low-pass filtered (moving average) with two different window lengths corresponding to the timescales chosen in SW06a, or (2) subject to the same wavelet decomposition described above.

[46] The method in SW06b was examined by applying it to a 2000-yearlong control integration (CTL) of the GISS model with constant forcings, where we know *a priori* that $\langle T \rangle$ varied independently of S. This simulation was used to test the crude method to estimate transfer functions, based on fractions of differences $\Delta \langle \overline{T} \rangle / \Delta \overline{S}$, where $\overline{x}$ was taken to be the mean value over a given century, and the Δ- operator was the difference between different centuries.

[47] A simple trend analysis was applied to the results, based on a linear regression between the temperature and time, providing a crude estimate of the magnitude of the long-term changes.

4.2. Results

[48] Figure 4 shows the wavelet components and the sinusoidal best fit for τ = 22 years. It is evident that the frequency band of the wavelet component is too broad to be well modeled with a simple expression like "$\frac{1}{2} A \sin(2\pi t)$," but using the expressions $A = 2\sqrt{(2)}\,\sigma$, we derived $A_{8,sun}$ = 0.32 Wm^{-2} and $A_{8,temp}$ = 0.18 K for 1900–2000 ($A_{8,sun}$ = 0.32 K Wm^{-2} and $A_{8,temp}$ = 0.16 K over the interval 1880–2002). SW05, on the other hand, got $A_{8,sun}$ = 0.35 ± 0.10 Wm^{-2} and $A_{8,temp}$ = 0.06 ± 0.01 K, but they based their analysis on the ACRIM *S* [*Willson and Mordvinov*, 2003] over the much shorter 1980–2002 period and used a global surface temperature from the Climate Research Unit, 2005 (they did not provide any reference to the data nor did they specify whether they used the combined land-sea data (HadCRUT) or land-only temperatures (CRUTEM).) These amplitudes are marked as shaded area around the original series in Figure 4. The middle panel also shows a comparison between the 0.06K amplitude (hatched inner area) compared with 0.18K (lighter solid shading), and our estimate (0.17K) is $2\sqrt{(2)}$ greater than their number when we use HADCRUT3v instead of GISTEMP.

[49] For τ = 11 years, our analysis gives $A_{7,sun}$ = 0.45 Wm^{-2} and $A_{7,temp}$ = 0.14 K (not shown), as opposed to $A_{7,sun}$ = 0.92 ± 0.05 Wm^{-2} and $A_{7,temp}$ = 0.10 ± 0.01 K in SW05. We also obtain $A_{7,temp}$ = 0.14 (not shown) if we repeat the analysis with HADCRUT3v data rather than GISTEMP.

[50] A change of 2 × 0.92 Wm^{-2} between solar minimum and maximum implies a change in S of 1.84 Wm^{-2} which amounts to 0.13% of S, and is greater than the ~0.08% difference between the peak and minimum of solar cycle 21 reported by *Willson* [1997] and the differences between TSI levels of the solar maxima and minima seen in this study (~1.2 Wm^{-2}; Figure 6). Furthermore, the difference in S between solar maximum and minimum cannot be explained in terms of a single wavelet component, but involves a superposition of several modes (not shown).

[51] We estimate Z_{22y} to be 0.55 K/[Wm^{-2}] using GISTEMP when taking the ratio of the standard deviations, or 0.58 K/[Wm^{-2}] using equations (5) and (6) (Figure 4), both of which were substantially higher than the value used in SW06a. Table 5 shows corresponding values derived when the GISTEMP $\langle T \rangle$ were replaced by global mean temperatures from the GCM runs. This way, we could test their method to see if it was able to discriminate between different forcings in data for which we knew *a priori* whether the solar forcing played a role or not. We used all the available data for these calculations as well as a common interval for S and $\langle T \rangle$ (1880–2000) and 1900–2000.

[52] In general, there are variations in the values for the coefficients, depending on the method from which they were estimated and on the time interval chosen. There is also a scatter between the different ensemble members within one ensemble, suggesting that the estimates are affected by intrinsic internal variations.

[53] The "GHG" experiments also give high values for Z_{22y}, even though it is known *a priori* that the results from these experiments are not influenced by the solar forcing. The value estimated for Z_{22y} using the ratio σ_T/σ_S was calculated to be 0.61 K/[Wm^{-2}] (0.31 K/[Wm^{-2}] using regression based on equations (5) and (6)) for "all," 0.82 K/[Wm^{-2}] (0.66 K/[Wm^{-2}]) for "GHG," and 0.11 K/[Wm^{-2}] (0.16 K/[Wm^{-2}]) for the "solar" experiment (Table 5). However, the individual ensemble members gave values ranging between 0.79 and 0.86 K/[Wm^{-2}] (0.51–0.78 K/[Wm^{-2}]) for the "GHG" experiment, whereas the results for "solar" were more similar to 0.17 K/[Wm^{-2}] from SW06a: 0.14–0.21 K/[Wm^{-2}] (0.14–0.40 K/[Wm^{-2}]).

[54] For Z_{11y}, the corresponding results were 0.38 K/[Wm^{-2}] (0.14 K/[Wm^{-2}]), 0.35 K/[Wm^{-2}] (0.13 K/[Wm^{-2}]), and 0.05 K/[Wm^{-2}] (0.03 K/[Wm^{-2}]) respectively (Table 5). These results suggest that the power seen in the bands chosen in SW05 and SW06a is influenced by long-term changes in F_{GHG}, and demonstrate that spurious results can easily occur. This is the same reason why the LCF results suggested intervals shorter than 11 years

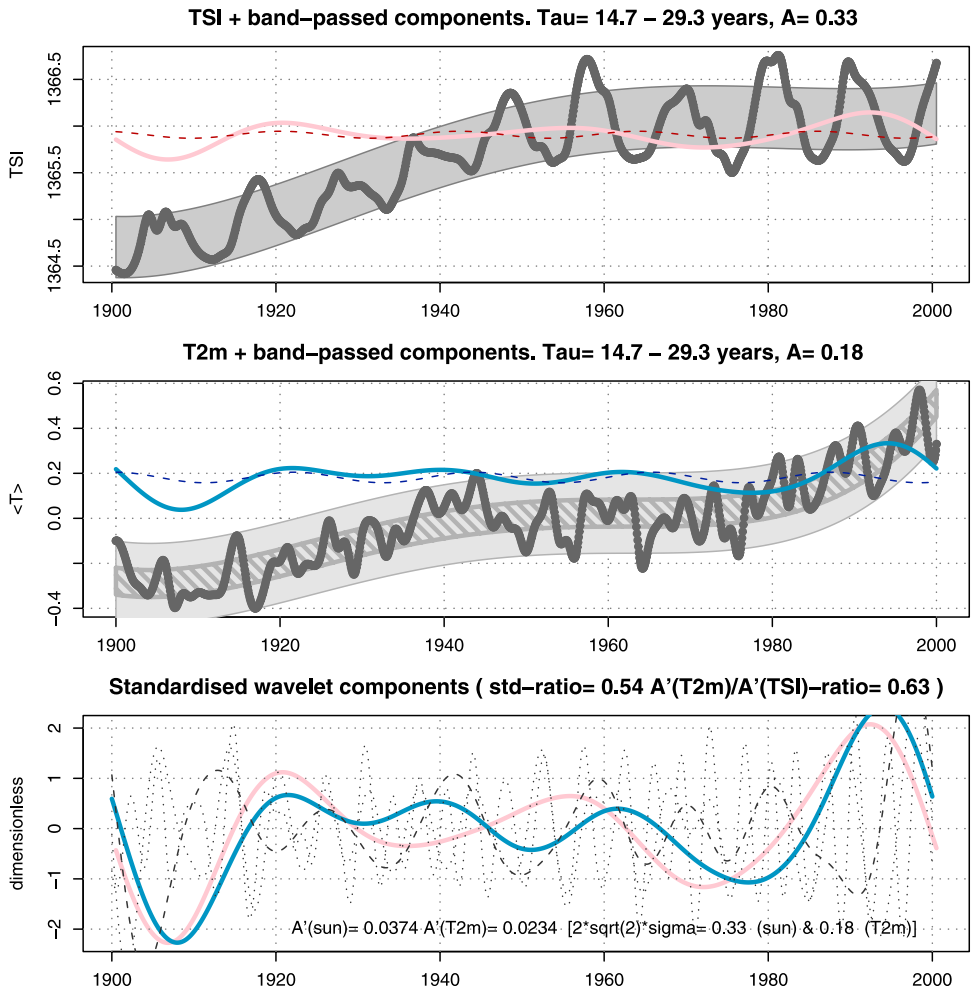

Figure 4. The (top) D_8 components of S (pink) and (center) $\langle T \rangle$ (blue) and best fit to equation (5) with period τ = 22 years (thin dashed lines). The original curves are shown in gray. (bottom) Standardized wavelet components D_8 for S (pink) and $\langle T \rangle$ (blue) together with D_5–D_7 for $\langle T \rangle$. The shaded area around the best fit 5th-order polynomial trend fits [*Benestad*, 2003] shows the magnitude of (top) $A_{8,\mathrm{sun}}$ and (center) $A_{8,\mathrm{temp}}$ relative to the time series. The hatched area in the center marks $A_{8,\mathrm{temp}}$ = 0.06 K.

between each correlation peak, and the regression coefficients were sensitive to the number of inputs in the regression analysis. Note that the values for Z_{11y} and Z_{22y} tend to be lower for the ensemble mean than for each realization of the "solar" runs, supporting the idea that there is a contamination from the internal variability (Table 5).

[55] We examined the SW06a method further by carrying out calculations based on equation (4). Three independent tests were carried out: (1) using an updated reconstruction of S [*Lean*, 2000]; (2) a recalculation of the *Scafetta and West* [2006a] curve for the PMOD composite with different values for the coefficients; and (3) repeating (2) using a different adjustment for matching the PMOD composite and the historic S reconstruction.

[56] Figure 5 shows the observed $\langle T \rangle$ together with values for $\langle \hat{T}_{sun} \rangle$ (t) for a number of different inputs for S and different choices for the adjustment between the observed irradiance and reconstructions prior to 1979. The curve reproducing SW06a (thin dark dashed) was almost identical to the curve in their Figure 3b. Any minor differences may be due to different ways of calculating lagged values and different length of series.

[57] The analysis using *Lean* [2000] rather than Scafetta and West's own solar proxy as input is shown as thick black lines. The thin dark short-dashed line shows results based on SW06a, but with a variation of their solar proxy using the mean value over the 17 common years of *Lean et al.* [1995] and PMOD to match the mean levels of these two data sets, rather than for just 1980. The curves were not critically sensitive to this choice of adjustment, but using the more recent *Lean* [2000] reconstruction gives substantially different results.

[58] Figure 6 shows different estimates for S compared to SW06a. There were some significant differences between the *Lean* [2000] reconstruction and the SW06a S reconstruction in the 1970s, during which the values from *Lean et al.* [1995] and the SW06a S were substantially lower than the more recent estimates [*Lean*, 2000]. In other words, the large difference between 1980 and the end of the time series reported by SW06a were due to lower values over one solar

Table 5. Values for Z_{22y} and Z_{11y} Estimated for the Different GCM Experiments Using Ratios of Standard Deviations (Left) the Ordinary Linear Regression (OLR) Approach of Equations (5)–(6) (Right)[a]

All data (S: 1610–2000; $\langle T \rangle$:1880–2003)						
Z_{11y} Emember	"All" σ_T/σ_S	"GHG"	"Solar"	"All" OLR	"GHG"	"Solar"
1	0.41	0.33	0.10	0.12	0.14	0.05
2	0.44	0.44	0.15	0.15	0.17	0.05
3	0.36	0.38	0.10	0.12	0.12	0.05
4	0.44	0.41	0.13	0.18	0.11	0.03
5	0.38	0.36	0.08	0.14	0.12	0.03
Emean	0.38	0.38	0.05	0.14	0.13	0.03
Z_{22y}	"All" σ_T/σ_S	"GHG"	"Solar"	"All" OLR	"GHG"	"Solar"
1	0.61	0.79	0.14	0.08	0.68	0.14
2	0.75	0.82	0.21	0.57	0.78	0.21
3	0.57	0.86	0.14	0.54	0.70	0.40
4	0.54	0.82	0.14	0.24	0.51	0.19
5	0.64	0.82	0.14	0.36	0.73	0.21
Emean	0.61	0.82	0.11	0.31	0.66	0.16
1880–2000						
Z_{11y} Emember	"All" σ_T/σ_S	"GHG"	"Solar"	"All" OLR	"GHG"	"Solar"
1	0.31	0.31	0.10	0.03	0.09	0.06
2	0.36	0.40	0.14	0.08	0.14	0.05
3	0.29	0.36	0.10	0.05	0.09	0.04
4	0.33	0.38	0.10	0.11	0.10	0.00
5	0.29	0.33	0.07	0.06	0.08	0.03
Emean	0.31	0.36	0.05	0.06	0.10	0.03
Z_{22y}	"All" σ_T/σ_S	"GHG"	"Solar"	"All" OLR	"GHG"	"Solar"
1	0.50	0.73	0.13	0.44	0.97	0.10
2	0.67	0.70	0.20	0.50	1.01	0.23
3	0.50	0.80	0.13	0.32	1.11	0.36
4	0.47	0.73	0.13	0.17	0.90	0.19
5	0.57	0.70	0.13	0.54	1.05	0.23
Emean	0.53	0.73	0.10	0.36	1.00	0.17
1900–2000						
Z_{11y} Emember	"All" σ_T/σ_S	"GHG"	"Solar"	"All" OLR	"GHG"	"Solar"
1	0.28	0.38	0.10	0.10	0.17	0.06
2	0.36	0.41	0.13	0.14	0.25	0.09
3	0.33	0.44	0.10	0.13	0.20	0.06
4	0.36	0.44	0.10	0.16	0.22	0.04
5	0.28	0.38	0.10	0.08	0.14	0.06
Emean	0.31	0.41	0.05	0.12	0.19	0.04
Z_{22y}	"All" σ_T/σ_S	"GHG"	"Solar"	"All" OLR	"GHG"	"Solar"
1	0.45	0.76	0.15	0.18	0.66	0.07
2	0.42	0.70	0.15	0.23	0.69	0.09
3	0.42	0.82	0.12	0.13	0.85	0.28
4	0.42	0.70	0.21	0.21	0.58	0.20
5	0.42	0.64	0.09	0.06	0.68	0.12
Emean	0.42	0.70	0.09	0.06	0.68	0.13

[a]Here, "Emember" refers to ensemble member, and "Emean" refers to results derived using the ensemble mean rather than individual runs. The coefficients have been estimated by taking all the available years, the maximum common interval (1880–2000), and the 1900–2000 period, and the large variations give an indication of how a little robust the method is.

cycle as well as a result of stitching together different types of data.

[59] Table 7 and Figure 5 provide trend estimates based on equation (4) and different S estimates, and all these are substantially less than the 25% suggested by SW06a: −7% to +10% of the total temperature increase since 1980, depending on the S used as input in equation (4). These estimates can be compared with the results from the multiple regression models in part 1, which suggest that S can explain an increase in $\langle T \rangle$ over the 20th century by ~0.1K, but no trend since 1980 (Figure 3).

[60] We also explore the sensitivity of the results to the choice of the parameters used in their model (equation (4)). Figure 7 shows the results of a sensitivity analysis carried out for different values for the parameters Z_{11y} and Z_{22y} in equation (4) (Table 6). The range of values for Z_{S4} in this sensitivity study was taken to reflect the spread of the null distributions of Z_{22y} derived from the Monte Carlo simulations (Figure 8).

[61] The character of the solutions is sensitive to the value for Z_{S4} (thin dashed lines; highlighted in bold in Table 6), for which Scafetta and West took to be similar to Z_{22y}, and less sensitive to the other coefficients. There is no known physical reason for why the climate sensitivity on secular scales should be lower than for 22-year scales, so it is fair to assume that $Z_{S4} \geq Z_{22y}$. Note that the estimates for Z_{22y} for the observations, shown in Figure 4 (0.55 K/[Wm^{-2}] or 0.58 K/[Wm^{-2}] for 1900–2000, depending on approach; corresponding values for 1885–2000 were 0.49 K/[Wm^{-2}] or 0.52 K/[Wm^{-2}] respectively), would yield unrealistic results with equation (4), as this these would imply values for Z_{S4} that are greater than the highest value highlighted in bold in Table 6 and predictions above the upper curve in Figure 7. In other words, these high values imply unrealistically high climate sensitivity.

[62] A spectral analysis (not shown) suggests that the 11-year cycles were more prominent in the solutions for equation (4) than in the observations, which had a stronger red noise character. The different spectral characteristics suggest that the estimation of coefficients Z_{11y} and Z_{22y}, by taking the relative magnitudes between two band-pass-filtered signals, does not identify a true connection between the two. These results therefore indicate that estimating Z_{11y} and Z_{22y} through the SW06a method is prone to noise contamination and produces spurious results, which is also implied from the LCF and regression analyses in part 1 of this study.

[63] A set of Monte Carlo simulations demonstrates that the ratio between the magnitudes of two similarly band-pass filtered random signals has a distribution with a considerable spread. These distributions are derived using the Monte Carlo simulations to mimic a random walk process or white noise in order to generate pairs of synthetic random data with similar mean and standard deviations to S and $\langle T \rangle$ respectively. The pairs of time series are, by construction, unrelated. Hence this exercise provides a null distribution and a way to examine the degree of uncertainty associated with such the method employed in SW05 and SW06a. The particular set up used here is arbitrary, but the conclusions are not sensitive to these choices. The ratios of standard deviations of the pairs of data were estimated for the band-pass-filtered series using wavelet analysis (Figure 8a) and white noise (Figure 8b), and by using a moving average to produce band-passed series from white noise (Figure 8c). In all these cases, a significant scatter is seen and values 0.11–0.21 used in SW06a are well within the null distribution.

[64] We applied the SW06b method to the long GISS CTL simulation (Figure 9) and found that this approach

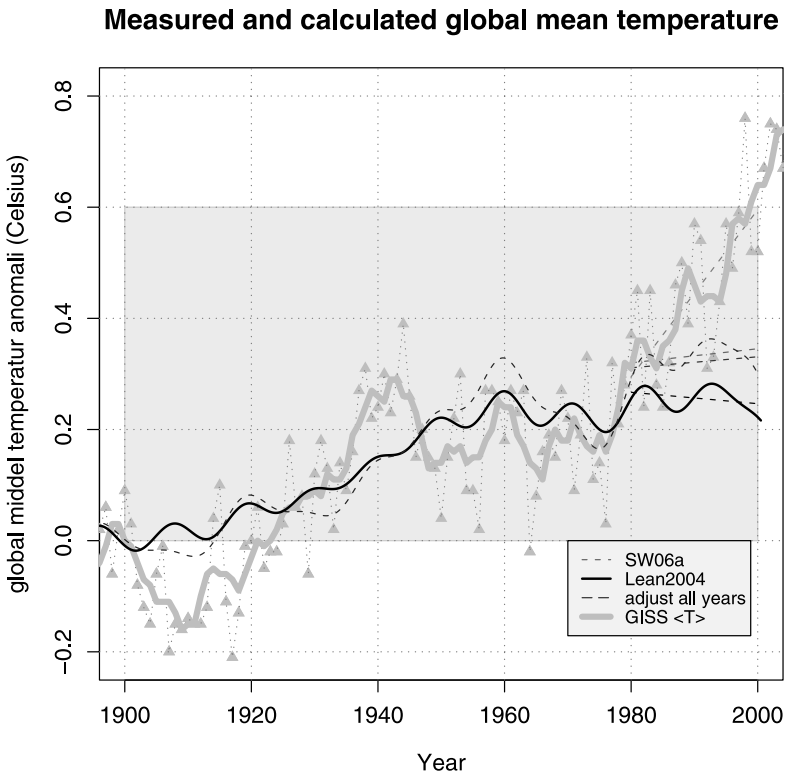

Figure 5. Observed $\langle T \rangle$ (5-year moving average and annual mean) and various solutions for T_{sun} using the SW06a method and their *S*, *Lean* [2000], and a *S* splice similar to the one in SW06a but using all 17 overlapping years for adjusting the *Lean et al.* [1995] *S* rather than just 1980. Linear trends after 1980 are shown as thin dashed lines (the values are shown in Table 7). Gray region corresponds to the axis ranges used in SW06a. The anomalies are departures from the 1900 value (using the 5-year moving average curve).

produced values of similar magnitude as the lower limits of the values reported in SW06b ($Z_{S,1} = 0.17 \pm 0.02 - 0.52 \pm 0.075$ K/[Wm^{-2}], $Z_{S,2} = 0.22 \pm 0.02 - 0.61 \pm 0.065$ K/[Wm^{-2}], and $Z_S = 0.20 \pm 0.03 - 0.57 \pm 0.075$ K/[Wm^{-2}], depending on the choice of solar reconstruction), even when we knew *a priori* that the $\langle T \rangle$ was not influenced by *S*. Figure 8d shows a histogram of values derived from CTL, and simple Monte Carlo simulations (not shown) further suggest a wide range for the null distribution for $\Delta \langle T \rangle / \Delta S$. The SW06b approach is also ill-posed when $\Delta S \rightarrow 0$ and $|\Delta \langle T \rangle| > 0$, and thus cannot be a generalizable approach.

5. Discussion

[65] The evaluation of the GISS ModelE $\langle T \rangle$ simulations, the LCF with solar forcing, and regression studies, suggest that the model approximately reproduces the observed statistical relationships between the global mean temperature and the solar and GHG forcings.

[66] The regression results reported above are only robust for strong forcings, and the values for α and β were consistent for "all" at 1-year lag (Tables 3 and 4), but the value for the solar forcing coefficient (β_1) was set to zero for the observations as the stepwise screening excluded solar forcings as input for the multiple regression.

[67] One explanation for the "all" experiment yielding a stronger solar-induced trend in $\langle T \rangle$ than seen in the observations may be that the GCM was too sensitive to solar forcing. However, another explanation may be that errors in the forcing estimate was exactly correct for the model (by construction), but may not be for the real world. Furthermore, the intrinsic variability also influences the estimates.

[68] We know *a priori* that the solar forcing coefficient (α_1) should be zero for the "GHG" ensemble, but the univariate regression produced $\hat{\alpha}_1 = 0.31 \pm 0.03$ K/[Wm^{-2}]. Negative values for α_1 were obtained for "residual" in the univariate analysis, however, the multiple regression against *S* and $ln|\rho|$ returned positive values. The value for the greenhouse gas coefficient (α_2) obtained from the "GHG" ensemble was substantially greater than for "all" and "obs" (Table 3), most likely due to the colinear negative aerosol forcing.

[69] Both F_S and F_{GHG} contain trends, and the different forcing components are not mutually orthogonal. Different ensemble members representing the same forced response but different realizations of intrinsic variability give different values for the solar and GHG regression coefficients. The linear regression analysis in part 1 was, however, unable to provide an exact description of the nonlinear response of the complicated climate system, due to the presence of colinearity in the forcings, internal chaotic variations, slow nonlinear response that may produce a more complete response after some time, or "leakage" between the different components [*Leroy*, 1998].

[70] Additionally, there may also be larger uncertainties in the forcing before 1958, which could affect the results for

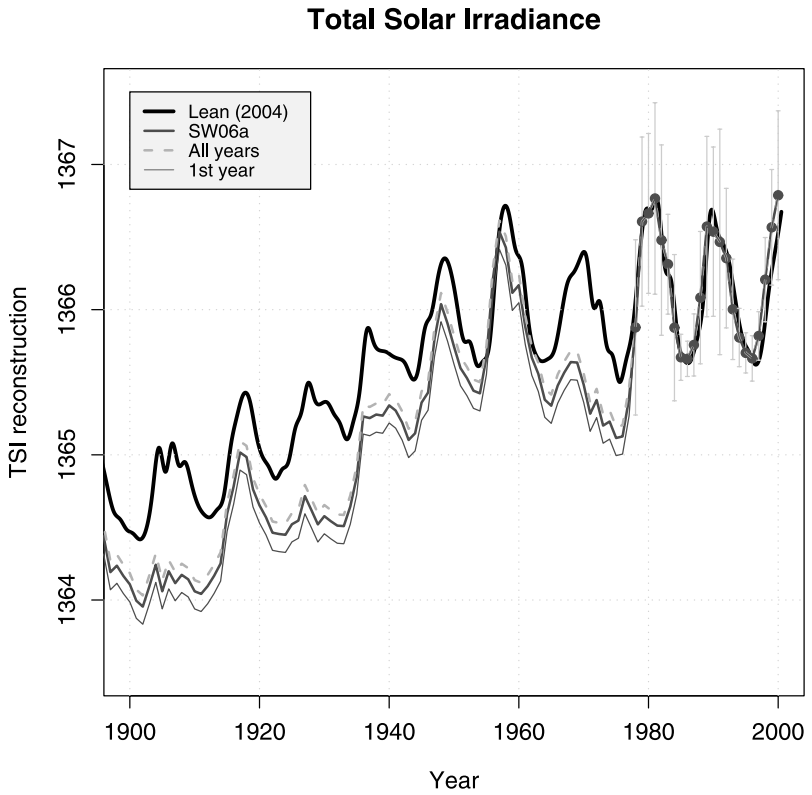

Figure 6. The reproduced SW06a *S* (dark gray) were similar to the curve in SW06a [Figure 2b]. The standard deviation of S for each year is shown as error bars for the satellite era, and a large scatter in *S* implies more uncertain estimates of the mean. Also shown are more recent estimates of *S* ([*Lean*, 2000] thick black).

the observations (though not for the numerical experiments). *Benestad* [2005] suggested that the sunspot record may have lower quality before 1900, as there was a dramatic change in the solar cycle length characteristics at around the start of the 20th century. Over the interval 1958–2000, the time series for *S* (little trend) and $\ln|\rho|$ were less colinear than over the 1880–2002 period. This may imply that the estimates based on equation (1) and the forcings over 1958–2000 may provide more reliable estimates of the sensitivity.

[71] The coefficient for greenhouse gases from the all-forcings multiple regression is $\hat{\beta}_2 = 0.91 \pm 0.19$ K/(Wm^{-2}), suggesting a climate sensitivity that is substantially greater than the equilibrium value reported for this model (0.67 K/(Wm^{-2})). Regression coefficients of $\hat{\alpha} \sim 0.45$ K/(Wm^{-2}), on the other hand, imply a transient climate sensitivity that is more consistent with the 1.5–1.6°C reported by *Solomon et al.* [2007].

[72] The values for solar and greenhouse gas forcing coefficients (α_1 and α_2) may in principle differ if they involve different feedback processes or if other mechanisms are involved. One example could be galactic cosmic rays (GCR) affecting low cloud cover [*Carslaw et al.*, 2002; *Dickinson*, 1975; *Ney*, 1959] or solar UV modifying the planetary wave propagation and heat distribution [*Shindell et al.*, 2001]. In these cases the forcing values might be underestimated, hence leading to an apparently larger sensitivity. However, the regression coefficients were similar for both GCM and observations, and the fact that these additional mechanisms were not present in these GISS ModelE simulations, suggest that processes such as GCR are not important, in agreement with *Sloan and Wolfendale* [2008] and *Kristjánsson et al.* [2008].

[73] It should be noted that the *p* values in Table 3 were estimated assuming independent and identically distributed (iid) data, but the presence of autocorrelation lowers the true degrees of freedom. Thus the true *p* values should be higher than those shown in the tables, and the true error bars should be wider. Furthermore, the regression analysis employed here does not yield robust results when additional forcing terms are included. Similarly, the fact that the regression did not pass the Durbin-Watson test for uncorrelated residuals, suggests that the regression was suboptimal. However, the purpose of using regression analysis here was simply to provide a means for comparing different data sets and studying their robustness.

[74] These results reveal the dangers in attributing characteristics of $\langle T \rangle$ to similar features in the forcings, and highlight the difficulties associated with detection and attribution more generally. We have also shown through the regression exercises that neglecting important forcings may inflate the climate sensitivity estimates since colinearity between different forcings interferes with the estimation of the sensitivity to each other. This is the main reason why the results produced by the methods in SW06a and SW06b are likely misleading. The key lessons are that detection and attribution has to include all factors (not just a single one)

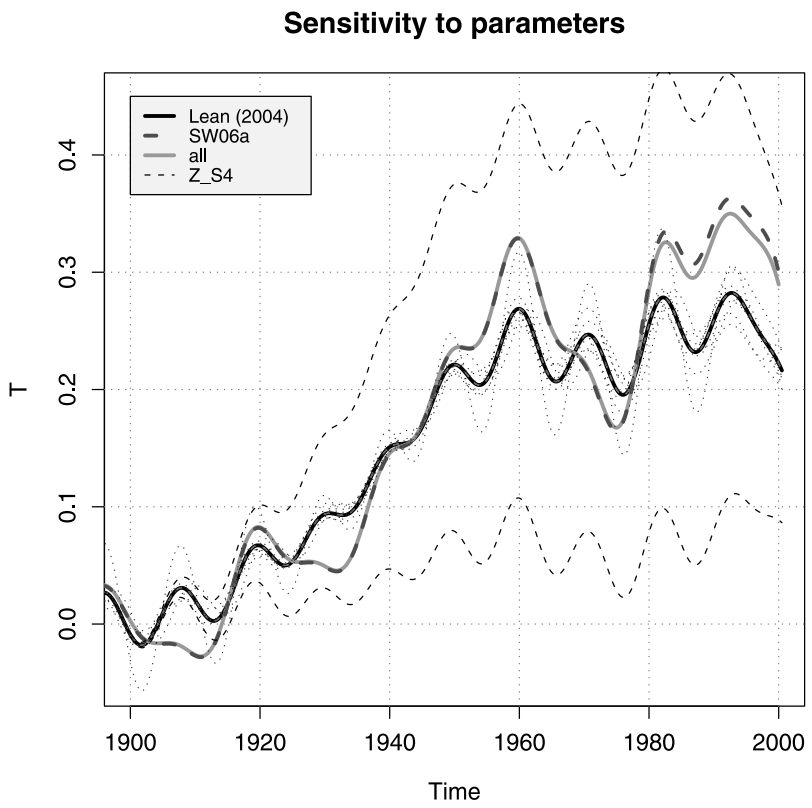

Figure 7. Sensitivity of the solution for $\langle \hat{T}_{sun} \rangle(t)$ to different values for the parameters listed in Table 6 and for different ways of combining PMOD and *Lean et al.* [1995] and *Lean* [2000] *S*.

and ensure that results are robust to different realizations of the intrinsic variability.

[75] There is an additional issue with the methodology of SW06a and that is the value they assume for the coefficient Z_{eq} This was taken as the ratio 288 K/(1365 Wm^{-2}) = 0.21 K/[Wm^{-2}]. The choice of this value determines the long-term sensitivity of the climate and is in fact the chief unknown; it can't simply be assumed. Taking this value as the absolute temperature divided by the total irradiance implies that climate change is linear from absolute zero to the present-day temperature, an assumption that is nowhere supported, and to our mind, extremely unlikely. Furthermore, the estimate Z_{eq} = 0.21 K/[Wm^{-2}] implies a climate sensitivity to the TOA radiative forcing of 4.5°C, and the climate sensitivities implied from SW06b were even higher. The adoption of such a high value as used by SW06a and SW06b, has a huge effect on their results.

[76] Variations in Z_{eq} can affect the long-term mean temperature, but not the trends directly. However, the value was used as an upper limit for the values for Z_{S4}, which had a direct bearing on the estimated trends. Spectral analyses and Monte Carlo experiments indicate that the strategy used in SW06a for estimating Z_{11y} and Z_{22y} is prone to noise contamination, thus producing possibly spurious and biased results. The values for Z_{22y} and Z_{11y} had been taken as the ratios between band-pass filtered values of global mean temperature and estimates for *S* representative for 22-year and 11-year timescales respectively, despite there being no direct correspondence between the two types of filtered curves [SW05, Figure 4]. In our emulation, we were not able to get exactly the same ratio of amplitudes, due to lack of robustness of the SW06a method and insufficient methods description. If our estimates for Z_{11y} and Z_{22y} were used as parameters in equation (4), we would get unrealistic values for $\langle \hat{T}_{sun} \rangle$ (*t*). Furthermore, the method fails to take the phase information into account, and a weak amplitude in the 22-year solar cycle was likely responsible for the spuriously high value for Z_{22y}. The lack of prominent spectral peaks in the power spectrum of observations and the presence of a spectral peak in the reconstructions also suggest that the values for the transfer coefficients were spuriously inflated.

Table 6. List Over Sensitivity Calculations With Equation (4) Using Different Values for the Parameters

Z_{eq}	Z_{s4}	Z_{22y}	Z_{11y}	t_{s4}	Z_4	Z_3
0.21	0.17	0.17	0.11	4.3	2.5	1.3
0.10	0.17	0.17	0.11	4.3	2.5	1.3
0.00	0.17	0.17	0.11	4.3	2.5	1.3
0.21	**0.05**	**0.17**	**0.11**	**4.3**	**2.5**	**1.3**
0.21	**0.30**	**0.17**	**0.11**	**4.3**	**2.5**	**1.3**
0.21	0.17	0.05	0.11	4.3	2.5	1.3
0.21	0.17	0.30	0.11	4.3	2.5	1.3
0.21	0.17	0.17	0.05	4.3	2.5	1.3
0.21	0.17	0.17	0.30	4.3	2.5	1.3
0.21	0.17	0.17	0.11	4.3	2.5	0.5
0.21	0.17	0.17	0.11	4.3	2.5	3
0.21	0.17	0.17	0.11	4.3	0.5	1.3
0.21	0.17	0.17	0.11	4.3	10	1.3
0.21	0.17	0.17	0.11	4.3	2.5	1.3

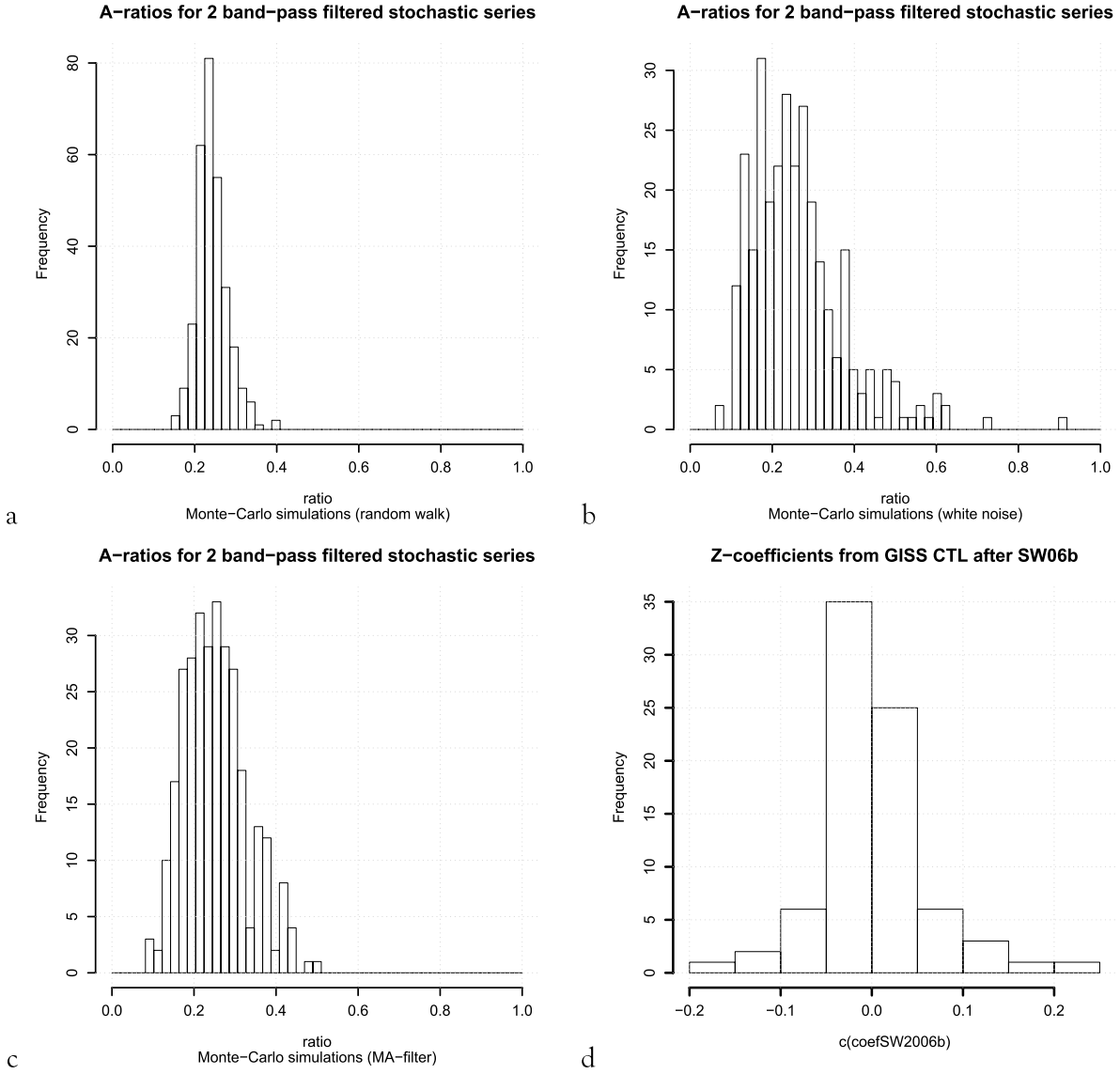

Figure 8. Null distribution for the SW06a and SW06b transfer functions for two cases wherein it is known *a priori* that there is no common signal. (a–c) Monte Carlo simulation of ratios of σ: (a) random walk and wavelet components [SW06a], (b) white noise and wavelet components [SW06a], and (c) band-pass filtered with moving average filters [SW06a]. (d) The SW06b ratios derived using $\langle T \rangle$ from CTL rather than actual observations.

[77] We showed above through Monte Carlo simulations that the ratio between the magnitudes of two similarly band-pass filtered random signals has a distribution with a considerable spread. The conclusions of SW06a therefore hinge on the assumption that none of the variance in the two frequency bands of the temperature was caused by other factors other than solar. This assumption is unlikely to hold.

[78] In an analogous way, the analysis of SW06b was based on the assumption that preindustrial variations in $\langle T \rangle$ could entirely be associated with changes in S. This will give an unrealistically high climate sensitivity, since other forcings, particularly volcanic, may also have played a significant role [*Shindell et al.*, 2004]. Additionally, the use of only one temperature reconstruction (for the northern hemispheric rather than global mean), underestimates the structural uncertainties in these estimates.

[79] There are additional issues concerning the analyses of Scafetta and West, even if the problematic parameter estimation for their models are ignored. One important difference between the solutions for $\langle \hat{T}_{sun} \rangle(t)$ here and in SW06a can be traced to low S values in the work of *Lean et al.* [1995] reconstruction between 1970 and 1980. Using the more recent *Lean* [2000] S there is no trend since 1980. Furthermore, they spliced the ACRIM Total Solar Irradiance (TSI) product to a TSI reconstruction based on reconstruction by *Lean et al.* [1995] or *Wang et al.* [2005] in such a way that the average reconstructed TSI value over 1980–1991 corresponded with the ACRIM mean for the same period. However, the different series

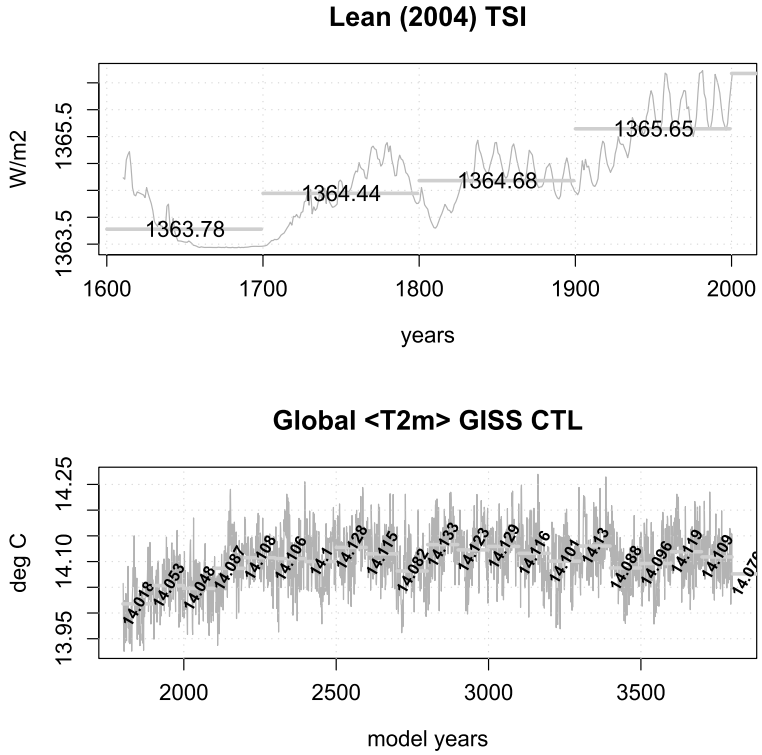

Figure 9. Comparison between centennial mean values for both *S* and GISS CTL. These time series are used to estimate the histogram in Figure 8d, showing rations derived from different combinations of the differences between the 100-year mean values.

had different trends over the same period, and stitching together data in such a simple fashion is likely to introduce nonhomogeneity.

[80] A discrepancy between $\langle \hat{T}_{sun} \rangle$ (t) and the global mean temperature is clearly apparent in Figure 5, where the temperature exhibits a local maximum around 1940, whereas $\langle \hat{T}_{sun} \rangle$ (t) peaks around 1960 for all solutions. Similar characteristics can also be seen in the figures of SW06a, although they were not discussed.

[81] It has been also established that this 1890–1930 "early century warming" was limited to the Arctic [*Johannessen et al.*, 2004] whereas the more recent warming has involved the whole latitudinal range. Thus a convincing solar warming hypothesis explaining both the warming periods would need to account for these different geographical fingerprints.

[82] Furthermore, SW06a did not carry out a proper trend analysis for estimating the increase in $\langle T \rangle$, but took the difference between instantaneous values of filtered data which also leads to a further inflation of their estimates. The purported low-end estimate of a 25% contribution from a solar origin since 1980 was not supported, as a proper trend analysis using a realistic reference level yields 8–10% when based on their strategy (Figure 5 and Table 7). If the *Lean* [2000] *S* were used instead of *Lean et al.* [1995], then the trend would be negative, thus more in line with *Lean* [2006].

[83] Scafetta and West proposed two mechanisms which may amplify the response to solar variations: (1) a purported effect of GCR on low cloud cover and hence the planetary albedo, or (2) changes in the solar UV radiation and a dynamic response to stratospheric warming [*Shindell et al.*, 2001; *Haigh*, 2003]. However, there is lack of a long-term trend in the GCR [*Lockwood and Fröhlich*, 2007; *Benestad*, 2005; *Richardson et al.*, 2002]. A more recent study suggests that GCR do not have an important effect on the cloud formation [*Sloan and Wolfendale*, 2008].

6. Conclusions

[84] We analyzed the GISS ModelE $\langle T \rangle$ in terms of its trend, LCF against solar forcing, and a set of regression analyses, and found that it gave a realistic reproduction of the observed global mean temperature. In particular, GISS ModelE simulates a response to solar and GHG forcings roughly consistent with the observations, but the exact

Table 7. Trend Estimates (the Proportion of the Total Warming Explained) and Standard Deviation Derived Using a Linear Model Between T_{sun} and Year Since 1980, Expressed in the Percentage of Similar Trend Analysis for the GISS Temperature[a]

	Lean [2000]	SW06	"All years"
Estimate	−7%	10%	8%
Stdv	±1.3%	±1.3%	±1.3%

[a]The trend estimates are shown as thin dashed lines in Figure 5, and "all years" refer to TSI reconstruction where the mean level for all overlapping years have been used to adjust the PMOD data rather than just 1980.

contribution from each forcing is difficult to pinpoint using statistical methods alone. Linear regression does not give unbiased and robust results if one tries to attribute the effect of different forcings on the temperature. The lack of robustness can also give rise to inflated values for the coefficients used in the statistical models of Scafetta and West. Nevertheless, variations in S appear to have a weak effect on the global mean temperature, but cannot explain the global warming since 1980.

[85] We also repeated the analyses of Scafetta and West, together with a series of sensitivity tests to some of their arbitrary choices. These tests showed clearly that the published uncertainty in their estimates was greatly underestimated. In particular, the arbitrary assumption of their equilibrium sensitivity (Z_{eq}) has a dramatic impact on their attribution of 20th century changes to solar forcing. We next showed that their methodologies were not able to robustly retrieve the solar contribution in GCM experiments where the answer was known *a priori*. In fact, we found that the presence of internal variability and additional forcings greatly confounded their method's accuracy. Even in much simpler cases, examined here using Monte Carlo simulations of synthetic climate time series, we found that their diagnostics had a very wide range in the absence of a true signal, so cannot be considered robust metrics of a solar-induced contribution.

[86] We conclude that as with the simpler linear regression methodologies described earlier, the SW methodology is highly sensitive to the internal variability of the climate system and the presence of colinear trends in different forcings. Given the concomitant increases in greenhouse gas forcings over the 20th century, this implies that their published attributions greatly exaggerate the role of solar variations in global mean temperature trends.

[87] Claims that a substantial fraction of post 1980 trends can be attributed to solar variations are therefore without solid foundation, and solar-related trends over the last century are unlikely to have been bigger than 0.1 to 0.2°C.

[88] **Acknowledgments.** We thank Urs Neu and Øyvind Nordli for valuable discussions. Part of the work has been supported by the Norwegian Research Council project "Norclim". All analyses were done in the R-environment version 2.8.0 [*Ihaka and Gentleman*, 1996], a statistical analysis tool freely available from http://cran.r-project.org.

References

Annan, J. D., and J. C. Hargreaves (2006), Using multiple observationally-based constraints to estimate climate sensitivity, *Geophys. Res. Lett.*, *33*, L06704, doi:10.1029/2005GL025259.

Bard, E., and G. Delaygue (2007), Comment on "Are there connections between the Earth's magnetic field and climate?" by V. Courillot, Y. Gallet, J.L. LeMouël, F., Fluteau, A. Genevey EPSL 253, 382, 2007, *Earth Planet Sci. Lett.*, *265*, doi:10.1016/j.epsl.2007.09.046.

Benestad, R. E. (2002), *Solar Activity and Earth's Climate*, Springer, Berlin.

Benestad, R. E. (2003), What can present climate models tell us about climate change?, *Clim. Change*, *59*, 311–332.

Benestad, R. E. (2005), A review of the solar cycle length estimates, *Geophys. Res. Lett.*, *32*, L15714, doi:10.1029/2005GL023621.

Brohan, P., J. J. Kennedy, I. Harris, S. F. B. Tett, and P. D. Jones (2006), Uncertainty estimates in regional and global observed temperature changes: A new dataset from 1850, *J. Geophys. Res.*, *111*, D12106, doi:10.1029/2005JD006548.

Camp, C. D., and K. K. Tung (2007), Surface warming by the solar cycle as revealed by the composite mean difference projection, *Geophys. Res. Lett.*, *34*, L14703, doi:10.1029/2007GL030207.

Carslaw, K. S., R. G. Harrison, and J. Kirkby (2002), Cosmic rays, clouds, and climate, *Science*, *298*, 1732–1737.

Dickinson, R. E. (1975), Solar variability and the lower atmosphere, *Bull. Am. Meteorol. Soc.*, *56*, 1240–1248.

Douglass, D. H., and B. D. Clader (2002), Climate sensitivity of the Earth to solar irradiance, *Geophys. Res. Lett.*, *29*(16), 1786, doi:10.1029/2002GL015345.

Foukal, P., C. Fröhlich, H. Spruit, and T. M. L. Wigley (2006), Variations in solar luminosity and their effect on the Earth's climate, *Nature*, *443*(7108), 161–166.

Fröhlich, C., and J. Lean (1998), The Sun's total irradiance: Cycles, trends and related climate change uncertainties since 1976, *Geophys. Res. Lett.*, *25*, 4377–4380.

Haigh, J. D. (2003), The effects of solar variability on the Earth's climate, *Philos. Trans. R. Soc. Lond. A*, *361*, 95–111.

Hansen, J., R. Ruedy, M. Sato, M. Imhoff, W. Lawrence, D. Easterling, T. Peterson, and T. Karl (2001), A closer look at United States and global surface temperature change, *J. Geophys. Res.*, *106*, 23,947–23,963.

Hansen, J., et al. (2005), Earth's energy imbalance: Confirmation and implications, *Science*, *308*, 1431–1435, doi:10.1126/science.1110252.

Hansen, J., Mki. Sato, R. Ruedy, K. Lo, D. W. Lea, and M. Medina-Elizade (2006), Global temperature change, *Proc. Natl. Acad. Sci.*, *103*, 14,288–14,293, doi:10.1073/pnas.0606291103.

Hansen, J., et al. (2007), Climate simulations for 1880–2003 with GISS modelE, *Clim. Dyn.*, *29*, 661–696.

Hegerl, G. C., F. W. Zwiers, P. Braconnot, N. P. Gillett, Y. Luo, J. A. Marengo Orsini, N. Nicholls, J. E. Penner, and P. A. Stott (2007), *Climate Change: The Physical Science Basis*, chap. Understanding and Attributing Climate Change, Cambridge Univ. Press, Cambridge, U. K.

IDAG (International ad hoc Detection and Attribution Group) (2005), Detecting and attributing external influences on the climate system: A review of recent advances, *J. Clim.*, *18*, 1291–1314.

Ihaka, R., and R. Gentleman (1996), R: A language for data analysis and graphics, *J. Comput. Graphic. Stat.*, *5*(3), 299–314.

Ingram, W. J. (2006), Detection and attribution of climate change, and understanding solar influence on climate, *Space Sci. Rev.*, *125*, 199–211, doi:10.1007/s11214-006-9057-2.

Johannessen, O. M., et al. (2004), Arctic climate change: Observed and modelled temperature and sea-ice variability, *Tellus A*, *56*, 328–341.

Kristjánsson, J. E., C. W. Stjern, F. Stordal, A. M. Fjæraa, G. Myhre, and K. Jónasson (2008), Cosmic rays, cloud condensation nuclei and clouds 2013 a reassessment using MODIS data, *Atmos. Chem. Phys.*, *8*, 7373–7387.

Krivova, N. A., L. Balmaceda, and S. K. Solanki (2007), Reconstruction of solar total irradiance since 1700 from surface magnetic flux, *Astron. Astrophys.*, *467*, 335–346.

Lean, J. (2000), Evolution of the Sun's spectral irradiance since the Maunder Minimum, *Geophys. Res. Lett.*, *27*, 2425–2428.

Lean, J. L. (2006), Comment on "Estimated solar contribution to the global surface warming using the ACRIM TSI satellite composite" by N. Scafetta and B. J. West, *Geophys. Res. Lett.*, *33*, L15701, doi:10.1029/2005GL025342.

Lean, J. L., and D. H. Rind (2008), How natural and anthropogenic influences alter global and regional surface temperatures: 1889 to 2006, *Geophys. Res. Lett.*, *35*, L18701, doi:10.1029/2008GL034864.

Lean, J., J. Beer, and R. Bradley (1995), Reconstruction of solar irradiance since 1610—implications for climate-change, *Geophys. Res. Lett.*, *22*, 3195–3198.

Leroy, S. S. (1998), Detecting climate signals: Some Bayesian aspects, *J. Clim.*, *11*, 640–651.

Lockwood, M., and C. Fröhlich (2007), Recent oppositely directed trends in solar climate forcings and the global mean surface air temperature, *Proc. R. Soc. A*, *463*, 2447–2460, doi:10.1098/rspa.2007.1880.

Lockwood, M., and C. Fröhlich (2008), Recent oppositely directed trends in solar climate forcings and the global mean surface air temperature: II. Different reconstructions of the total solar irradiance variation and dependence on response time scale, *Proc. R. Soc.*, *464*, 1367–1385, doi:10.1098/rspa.2007.0347.

Myhre, G., E. J. Highwood, K. P. Shine, and F. Stordal (1998), New estimates of radiative forcing due to well mixed greenhouse gases, *Geophys. Res. Lett.*, *25*, 2715–2718.

Ney, E. P. (1959), Cosmic radiation and the weather, *Nature*, *183*, 451–452.

Richardson, I. G., E. W. Cliver, and H. V. Cane (2002), Long-term trends in interplanetary magnetic field strength and solar wind structure during the twentieth century, *J. Geophys. Res.*, *107*(A10), 1304, doi:10.1029/2001JA000507.

Scafetta, N., and B. J. West (2005), Estimated solar contribution to the global surface warming using the ACRIM TSI satellite composite, *Geophys. Res. Lett.*, *32*, L18713, doi:10.1029/2005GL023849.

Scafetta, N., and B. J. West (2006a), Phenomenological solar contribution to the 1900–2000 global surface warming, *Geophys. Res. Lett.*, *33*, L05708, doi:10.1029/2005GL025539.

Scafetta, N., and B. J. West (2006b), Phenomenological solar signature in 400 years of reconstructed Northern Hemisphere temperature record, *Geophys. Res. Lett.*, *33*, L17718, doi:10.1029/2006GL027142.

Scafetta, N., and B. J. West (2007), Phenomenological reconstructions of the solar signature in the Northern Hemisphere surface temperature records since 1600, *J. Geophys. Res.*, *112*, D24S03, doi:10.1029/2007JD008437.

Scafetta, N., and B. J. West (2008), Is climate sensitive to solar variability?, *Phys. Today*, *3*, 50–51.

Scafetta, N., and R. C. Willson (2009), ACRIM-gap and TSI trend issue resolved using a surface magnertic flux TSI proxy model, *Geophys. Res. Lett.*, *36*, L05701, doi:10.1029/2008GL036307.

Schmidt, G. A., et al. (2006), Present day atmospheric simulations using GISS ModelE: Comparison to in-situ, satellite and reanalysis data, *J. Clim.*, *19*, 153–192, doi:10.1175/JCLI3612.1.

Shindell, D. T., G. A. Schmidt, R. L. Miller, and D. Rind (2001), Northern Hemipshere winter climate response to greenhouse gas, ozone, solar, and volcanic forcing, *J. Geophys. Res.*, *106*, 7193–7210.

Shindell, D. T., G. A. Schmidt, R. L. Miller, and M. E. Mann (2004), Volcanic and solar forcing of climate change during the predindustrial era, *J. Clim.*, *16*, 4094–4107.

Sloan, T., and A. W. Wolfendale (2008), Testing the proposed causal link between cosmic rays and cloud cover, *Environ. Res. Lett.*, *3*, 024001.

Solomon, S., D. Quin, M. Manning, Z. Chen, M. Marquis, K. B. Averyt, M. Tignotr, and H. L. Miller (Eds.) (2007), *Climate Change: The Physical Science Basis. Contribution of Working Group I to the Fourth Assessment Report of the Intergovernmental Panel on Climate Change*, Cambridge Univ. Press, Cambridge, U. K.

Stott, P. A., S. F. B. Tett, G. S. Jones, M. R. Allen, W. J. Ingram, and J. F. B. Mitchell (2001), Attribution of twentieth century temperature change to natural and anthropogenic causes, *Clim. Dyn.*, *17*, 1–21.

Wang, Y.-M., J. L. Lean, and N. R. Sheeley (2005), Modeling the Sun's magnetic field and irradiance since 1713, *Astrophys. J.*, *625*, 522–538.

Wigley, T. M. L. (1988), The climate of the past 10,000 years and the role of the Sun, in *Secular Solar and Geomagnetic Variations in the Last 10,000 Years: Proceedings*, edited by F. R. Stephenson and A. W. Wolfendale, pp. 209–224, Springer, New York.

Wilks, D. S. (1995), *Statistical Methods in the Atmospheric Sciences*, Acad. Press, Orlando, Fla.

Willson, R. C. (1997), Total solar irradiance trend during solar cycles 21 and 22, *Science*, *277*(5334), 1963–1965.

Willson, R. C., and A. V. Mordvinov (2003), Secular total solar irradiance trend during solar cycles 21–23, *Geophys. Res. Lett.*, *30*(5), 1199, doi:10.1029/2002GL016038.

R. E. Benestad, Climate Division, Norwegian Meteorological Institute, P.O. Box 0313, Oslo, Norway. (rasmus.benestad@met.no)

G. A. Schmidt, NASA Goddard Institute for Space Studies, 2880 Broadway, New York, NY 10025, USA. (gschmidt@giss.nasa.gov)